Positron collisions with ethene

Márcio H. F. Bettega,[1] Sergio d'A. Sanchez,[1] Márcio T. do N. Varella,[2] Marco A. P. Lima,[3] Luca Chiari,[4,5] Antonio Zecca,[5] Emanuele Trainotti,[5] and Michael J. Brunger[4,6]

[1]*Departamento de Física, Universidade Federal do Paraná, Caixa Postal 19044, 81531-990 Curitiba, Paraná, Brazil*

[2]*Instituto de Física, Universidade de São Paulo, Caixa Postal 66318, 05315-970 São Paulo, SP, Brazil*

[3]*Instituto de Física Gleb Wataghin, Universidade Estadual de Campinas, Caixa Postal 6165, 13083-970 Campinas, SP, Brazil*

[4]*ARC Centre for Antimatter-Matter Studies, School of Chemical and Physical Sciences, Flinders University, GPO Box 2100, Adelaide, South Australia 5001, Australia*

[5]*Department of Physics, University of Trento, Via Sommarive 14, I-38123 Povo (Trento), Italy*

[6]*Institute of Mathematical Sciences, University of Malaya, 50603 Kuala Lumpur, Malaysia*

(Received 3 July 2012; revised manuscript received 24 July 2012; published 15 August 2012)

We present experimental and theoretical cross sections for positron collisions with ethene molecules. The experimental total cross sections (TCSs) were obtained with a linear transmission technique, for energies from 0.1 eV up to 70 eV. The calculations employed the Schwinger multichannel method and were performed in the static plus polarization approximation for energies up to 10 eV. Our calculated elastic cross sections indicate a Ramsauer-Townsend minimum around 2.8 eV and a virtual state, in agreement with previous calculations by da Silva *et al.* [Phys. Rev. Lett. **77**, 1028 (1996)]. We found reasonable agreement between the calculated elastic integral cross section and the measured total cross section below the positronium formation threshold. The present results are also in quite good agreement with available theoretical and experimental data, although for the experiments this is only true for TCSs above about 7 eV.

DOI: 10.1103/PhysRevA.86.022709 PACS number(s): 34.80.Uv, 34.80.Bm

I. INTRODUCTION

Positron physics has gained considerable interest in recent years due to experimental advances that have allowed for more intense and monoenergetic positron beams (see [1] for a review). However, agreement among theoretical and experimental data obtained by different groups is still not particularly satisfactory, even for the total cross section (TCS) of simple targets [2–4]. Further improvements in scattering models and experimental techniques would thus be desirable.

Ethene is a small hydrocarbon (see Fig. 1) that has been the subject of several studies of low energy electron and positron collisions. In the case of electron interactions with ethene, there is a Ramsauer-Townsend minimum at around 0.1 eV and a π^* shape resonance at around 2 eV in the elastic cross sections of the B_{2g} symmetry. In general, the comparison between the different calculations and experiments shows that they agree well with each other [6]. This molecule has also been used as a prototype to investigate the influence of polarization effects on the electronic excitation of low-lying triplet states [7].

There are also experimental [8,9] and theoretical [10–13] studies addressing positron collisions with ethene. Although the experimental data agree relatively well for energies above ~7 eV, they differ in magnitude for lower energies. Previous calculations reported by da Silva *et al.* [10,13] pointed out the existence of a Ramsauer-Townsend minimum around 2 eV, and were in good agreement with the experimental data available at the time [9]. Occhigrossi and Gianturco [12] also reported elastic integral cross sections and annihilation parameter (Z_{eff}) estimates for positron collisions with ethene, although they did not discuss the Ramsauer-Townsend minimum.

In more recent studies, ethene was shown as a useful prototype system to understand the role of multiquantum vibrational excitations (combination vibrations and overtones) in resonant positron annihilation. Due to the many infrared (IR) inactive vibrations of the ethene molecule, positron attachment into bound or virtual states cannot be accounted for solely by the dipole interaction [14] (the dipole potential only couples IR active vibrations), and the inclusion of correlation-polarization effects would be essential to describe the resonance spectrum of ethene [15,16]. As the comparison of calculated cross sections with experimental data is invaluable to assess the accuracy of polarization models, scattering studies may be helpful to improve the resonant annihilation models.

The present paper reports experimental total cross sections and theoretical elastic integral cross sections (ICS) for positron scattering by ethene. The experiment was based on a linear transmission technique [3], covering the positron energies from 0.1 to 70 eV. The calculated fixed-nuclei elastic cross sections (not accounting for positronium formation) were obtained with the Schwinger multichannel method [17,18] at very low collision energies, up to 10 eV. The description of polarization effects has been improved with respect to the previously reported calculations by da Silva *et al.* [10,13]. The goal of this paper is to present a set of new results for this molecule and to provide a systematic comparison between the results available in the literature.

The remainder of this paper is organized as follows. In Sec. II we present the experimental details. Section III discusses the theoretical approach and the computational details employed in our calculations. The results are presented and discussed in Sec. IV, while a brief summary of our findings ends the paper.

II. EXPERIMENTAL DETAILS

The present measurements were carried out with a positron apparatus developed by Zecca and collaborators, which has already been described in detail in a previous paper [3]. Hence,

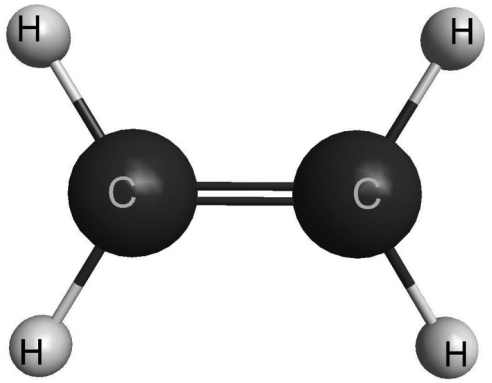

FIG. 1. Geometrical structure of C_2H_4. Generated using MACMOLPLT [5].

we just recall here that it is based on a linear transmission technique and that the positron beam is produced from a radioactive ^{22}Na isotope (activity of ∼1.4 mCi at the time of the present measurements), in conjunction with a 1 μm-thick tungsten moderator [19] and a set of electrostatic optics. As a standard practice, the moderator has been re-conditioned before measuring this target.

In our experiments the beam intensity is attenuated as a consequence of the incident positrons interacting (or not) with the ethene molecules, as described by the Beer-Lambert law:

$$I_1 = I_0 \exp\left[\frac{-(P_1 - P_0)L\sigma}{kT}\right]. \quad (1)$$

According to Eq. (1) it is possible to determine the TCS of interest (σ) from measurements of the positron beam count rate with and without the ethene gas in the scattering region (I_1 and I_0, respectively). We also need to measure the pressure in the scattering cell with ethene routed to the scattering region, and then the pressure when ethene is diverted into the vacuum chamber [i.e., away from the scattering chamber (P_1 and P_0, respectively)]. The temperature of the ethene gas in the scattering cell (T) is measured by a platinum (PT100) resistance thermometer in thermal contact with the scattering chamber. The length of the scattering cell in our experimental configuration is $L = 22.1 \pm 0.1$ mm. Finally, in Eq. (1), k is the Boltzmann constant.

Several experimental precautions need to be taken when carrying out the measurements. These include minimizing double scattering events, a condition that is fulfilled by setting the target pressure in the scattering cell such that the beam attenuation (i.e., the ratio I_1/I_0) is greater than 0.7. In addition, note that only a high-purity ethene source (>99.9% from BOC gases) was used throughout the present measurements. As a standard practice in our laboratory, in order to check for the validity of our techniques and procedures, before any experiment on a new target is started we make preliminary validation measurements using targets for which the positron scattering TCSs are considered well known. Such well-characterized systems might be drawn from the noble gases [20–22] and molecular nitrogen [3].

When undertaking measurements at very low energies, like in the present study, it is crucial for the energy scale to be calibrated accurately. The zero for the incident positron energy scale was determined here with a retarding potential analysis (RPA) of the beam, without the target gas in the vacuum chamber, as outlined in [23]. We estimate the error on the energy scale to be ±0.05 eV in this case. The same RPA allows us to also measure the energy distribution of the beam [23] and thus its energy resolution. The energy width of the beam was found to be ∼0.25 eV (full width at half maximum) for these measurements, with an uncertainty of ±0.05 eV at most. As in all spectroscopies, our measured cross sections are actually the convolution of the "real TCSs" with the beam energy distribution. This physically means that, once corrected for this effect, the "real TCSs" should be somewhat larger in magnitude than what we measure. However, this correction is expected to be significant only at very low energies (below ∼0.5 eV), where the positron energy becomes comparable to the beam width itself.

The measured data also need to be corrected for some instrumental effects that inevitably affect the measurements, before they can be used in Eq. (1). For instance, the length of the scattering region (L) needs to be corrected to account for the increase in the positrons path length due to the gyration of the particles in the focusing axial magnetic field present in the scattering region. As the magnetic field was $B \sim 11$ G in the present measurements, for positron energies between 0.1 and 32.5 eV, the value of L increased by 5.5%. For incident energies between 35 and 70 eV the magnetic field was decreased to $B \sim 4$ G, and hence the increase in L was just 2%. In addition, the pressure measurements also need to be corrected to account for the thermal transpiration effect. In fact, the pressure readings were achieved with an MKS 627B capacitance manometer operating at 45 °C, whereas the ethene gas in the scattering cell was held at $T = 64 \pm 2$ °C (note that the vacuum chamber was warmed during the measurements). In this case the thermal transpiration correction was made by following the semiempirical model of Takaishi and Sensui [24] and resulted in a maximum decrease in the absolute value of the TCS of ∼3%.

Like all scattering cell-based linear transmission experiments, the present experiment suffers from angular discrimination limitations. They stem from the inability of the detector to distinguish between the positrons that are elastically scattered at very forward angles from those of the primary (unscattered) beam. This effect results in the scattered positron count rate being somewhat overestimated, and therefore, the measured TCSs are somewhat smaller in magnitude than their "true values." At any given energy, the extent of the forward angle scattering effect depends on the angular discrimination of the apparatus and on the nature of the elastic differential cross sections (DCSs) for the target in question in this forward angle region [25]. From the geometry of the scattering and detection regions, the angular acceptance of the Trento apparatus is estimated to be $\Delta\theta \sim 4°$ [3]. This value compares favorably with that from the spectrometers at Wayne State University ($\Delta\theta \sim 16°$) [26], Yamaguchi University ($\Delta\theta \sim 7°$), and Bielefeld University ($\Delta\theta \sim 5.7°$) [8], while it is close to that achieved at the Australian National University (see, e.g., [27]). However, it is also known [28] that the gyration of the positrons can also potentially increase the angular discrimination error compared to the no-field case. Using some of the equations detailed in Kauppila *et al.* [26], but for the typical conditions of

TABLE I. Present measured TCSs for positron scattering from ethene. The errors given represent the statistical component of the overall uncertainty only.

Energy (eV)	TCS (10^{-20} m^2)	TCS error (10^{-20} m^2) ($\pm1\sigma$)	Energy (eV)	TCS (10^{-20} m^2)	TCS error (10^{-20} m^2) ($\pm1\sigma$)
0.10	127.83	7.45	6.50	20.30	0.48
0.15	106.52	3.72	7.00	20.43	0.20
0.20	93.93	2.27	7.50	20.27	0.27
0.30	78.77	2.47	8.00	20.20	0.34
0.40	66.92	1.38	9.00	19.93	0.41
0.50	59.26	1.54	10.00	19.51	0.52
0.60	54.99	1.07	12.50	18.54	0.35
0.70	50.70	0.95	15.00	18.37	0.22
0.80	46.93	2.98	17.50	17.80	0.41
1.00	40.34	1.27	20.00	17.74	0.23
1.25	36.61	0.99	22.00	17.77	0.31
1.50	32.96	1.25	25.00	17.07	0.46
1.75	29.76	0.19	27.00	16.79	0.18
2.00	26.51	0.69	30.00	16.75	0.54
2.50	23.35	0.46	32.50	16.56	0.58
2.75	22.35	0.18	35.00	16.04	0.59
3.00	21.50	0.19	40.00	15.74	0.21
3.25	20.41	0.38	45.00	15.54	0.52
3.50	20.27	0.28	50.00	15.91	0.39
4.00	20.24	0.44	55.00	15.01	0.33
4.50	20.13	0.57	60.00	14.63	0.25
5.00	19.79	0.59	70.00	13.98	0.07
6.00	20.14	0.38			

our experiments, the energy-dependent angular discrimination to be associated with the gyration of the particles in the present apparatus was evaluated to vary between 17.5° at 1 eV and 2.4° at 50 eV positron energy (see Table 2 in Zecca *et al*. [3]). These angular discrimination values, as a function of the positron energy, can then in principle be used in conjunction with the appropriate elastic DCSs, at the same energy, provided that these are known, to correct the measured TCSs for the forward angle scattering effect. This can be done by following the approach described, for instance, in Hamada and Sueoka [28]. In principle, such DCSs are available from our SMC-level calculations (see next section). However, given that our experimental TCS and the present computed elastic ICS agree only qualitatively, as we shall see later in our results and discussion section, at this time employing those DCSs in the manner outlined above might be a little premature and so we have in general not done so. Therefore, the TCSs we present here (see Table I) are underestimated with respect to their "true values." Nonetheless, to illustrate the forward angle discrimination effect we have employed the theoretical elastic differential cross sections (see Sec. III) at 0.1, 0.5, 1, 5, and 10 eV (see Fig. 2 and Table II) to obtain estimates of TCS corrections that we might expect at those energies. We find that the magnitude of the TCS we list in Table I increases by ∼39% at 0.1 eV, 16% at 0.5 eV, 12% at 1 eV, 4% at 5 eV, and 2% at 10 eV. Those corrected TCSs are also plotted in the lower panel of Fig. 3, where we also see that the effect is clearly bigger at the lowest energy and becomes smaller as one goes to the higher energies.

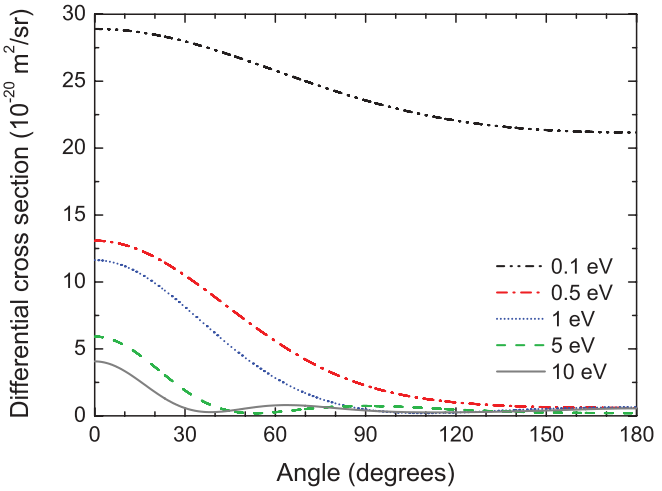

FIG. 2. (Color online) Present positron-ethene theoretical elastic differential cross sections for incident positron energies of 0.1, 0.5, 1, 5, and 10 eV. See legend in the figure for further details.

The present measurements on ethene span the energy range between 0.1–70 eV. The statistical uncertainties on the data amount to 2.3% on average, but were found to remain between 1.1% and 3.5% throughout the investigated energy range. Note that the largest errors are usually found at the lowest energies. This is associated with a decrease of the beam intensity when decreasing the positron energy. The overall uncertainties on the TCSs are estimated to be within the 5%–12% range. They originate from the quadrature combination of quantities like the statistical uncertainties, the uncertainty in the thermal transpiration corrections (<2%), the uncertainty in the value of the length of the scattering region and its correction for the effective positron path length (<3%), and the uncertainties in the pressure and temperature readings (<1% each).

TABLE II. Present theoretical elastic differential cross sections (in units of 10^{-20} m^2/sr) for positron scattering from ethene.

Angle (°)	0.1 eV	0.5 eV	1 eV	5 eV	10 eV
0	28.90	13.09	11.63	5.92	4.07
10	28.79	12.76	11.18	5.26	3.34
20	28.47	11.85	9.91	3.65	1.78
30	27.97	10.49	8.12	1.89	0.58
40	27.33	8.86	6.16	0.68	0.28
50	26.58	7.17	4.34	0.22	0.55
60	25.79	5.58	2.82	0.27	0.78
70	25.00	4.21	1.69	0.51	0.76
80	24.25	3.10	0.93	0.69	0.58
90	23.56	2.26	0.47	0.74	0.40
100	22.96	1.67	0.26	0.69	0.30
110	22.46	1.26	0.20	0.58	0.26
120	22.06	1.00	0.25	0.47	0.27
130	21.74	0.83	0.34	0.37	0.29
140	21.51	0.72	0.44	0.30	0.34
150	21.35	0.65	0.52	0.25	0.40
160	21.24	0.61	0.59	0.22	0.47
170	21.19	0.59	0.62	0.21	0.53
180	21.17	0.59	0.64	0.20	0.56

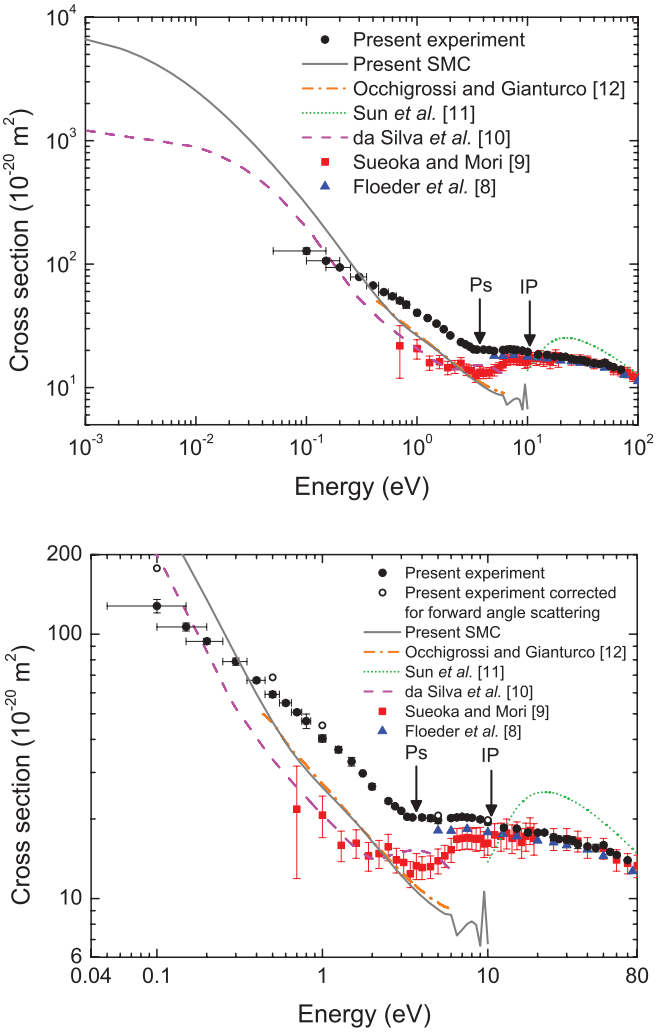

FIG. 3. (Color online) (Top panel) Cross sections for positron collisions with ethene. Circles (black), present TCS; solid line (gray), present elastic ICS; dotted line (green), results from [11]; triangles (blue), results from [8]; squares (red), results from [9]; dot-dashed line (magenta), ICS from [10]; dashed line (orange), ICS from [12]. (Lower panel) Same as top panel, in a smaller scale, except that here we have also, at 0.1, 0.5, 1, 5, and 10 eV, included the present TCSs corrected for the forward angle scattering effect (using our theoretical differential cross sections), open circles (black). See text for discussion.

III. THEORY

The elastic cross sections were computed with the Schwinger multichannel method (SMC) [29] as implemented for positron-molecule collisions. This method has been described in detail in several publications [17,18], so here we will only discuss those points that are relevant to the present calculations.

The working expression for the scattering amplitude is

$$f(\vec{k}_f,\vec{k}_i) = -\frac{1}{2\pi}\sum_{m,n}\langle S_{\vec{k}_f}|V|\chi_m\rangle(d^{-1})_{mn}\langle\chi_n|V|S_{\vec{k}_i}\rangle, \quad (2)$$

where

$$d_{mn} = \langle\chi_m|A^{(+)}|\chi_n\rangle, \quad (3)$$

and

$$A^{(+)} = Q\hat{H}Q + PVP - VG_P^{(+)}V. \quad (4)$$

In the above equations, $|S_{\vec{k}_{i,f}}\rangle$ is a solution of the unperturbed Hamiltonian H_0 (the kinetic energy of the incoming positron plus the target Hamiltonian) and is a product of a target state and a plane wave, V is the interaction potential between the incident positron and the electrons and nuclei of the target, $|\chi_m\rangle$ is a set of $(N+1)$-particle configuration state functions (CSFs) used in the expansion of the trial scattering wave function, $\hat{H} = E - H$ is the collision energy minus the full Hamiltonian of the system ($H = H_0 + V$), P is a projection operator onto the open-channel space defined by the target eigenfunctions, and $G_P^{(+)}$ is the free-particle Green's function projected onto the P space. Finally $Q = (\mathbb{1} - P)$ is the projector onto the closed electronic channels of the target.

The direct space is composed by CSFs of the form,

$$|\chi_j\rangle = |\Phi_1\rangle \otimes |\varphi_j\rangle, \quad (5)$$

where $|\Phi_1\rangle$ represents the ground state of the molecule obtained at the Hartree-Fock (HF) level and $|\varphi_j\rangle$ is a single-particle orbital used to expand the positron scattering orbital (see below). Polarization effects are incorporated by augmenting the direct space with CSFs of the closed space constructed as

$$|\chi_{ij}\rangle = |\Phi_i\rangle \otimes |\varphi_j\rangle, \quad (6)$$

where $|\Phi_i\rangle$ is obtained from virtual single excitations of the target out of the HF reference state.

Our present calculations were performed in the static plus polarization approximation in the D_{2h} symmetry group. We used the ground-state equilibrium geometry of the ethene molecule given in Ref. [10] and the single-particle basis described in Ref. [30], except for the p-type function on the hydrogens, whose exponent is 0.2 in the present calculations. The geometrical structure of C_2H_4 is shown in Fig. 1.

Polarization effects were taken into account through single excitations of the target from the hole (occupied) orbitals to a set of particle (unoccupied) orbitals. Here we considered the six outermost occupied orbitals as hole orbitals. To represent the particle orbitals we employed the 80 lowest improved virtual orbitals (IVOs) [31]. These IVOs, along with the eight occupied orbitals, were used as scattering orbitals. We thus obtained 6311 CSFs for the A_g symmetry, 5963 CSFs for the B_{3u} symmetry, 4622 CSFs for the B_{2u} symmetry, 4280 CSFs for the B_{1g} symmetry, 6311 CSFs for the B_{1u} symmetry, 5963 CSFs for the B_{2g} symmetry, 4622 for the B_{3g} symmetry, and 4280 CSFs for the A_u symmetry. The total of 42,352 CSFs is almost twice the number of CSFs employed in the previous calculation of Ref. [10].

IV. RESULTS

The top panel of Fig. 3 shows our present experimental TCS and theoretical elastic ICS in comparison with the data from Sueoka and Mori [9] and from Floeder *et al.* [8], as well as calculations from Sun *et al.* [11], da Silva *et al.* [10], and of Occhigrossi and Gianturco [12]. In this figure the threshold for positronium formation (P_s) of 3.7 eV and the first ionization potential (IP) of 10.5 eV [32] are indicated by vertical arrows.

The relationship between these two quantities is $P_s = \mathrm{IP} - 6.8$ (in eV). The opening of these scattering channels can be seen in the experimental data as changes in the slope of the total cross section in the proximity of these energies. None of the theories consider positronium formation explicitly. Hence, we do not expect very good agreement between our theoretical results and the experimental data above 3.7 eV. In fact, from Fig. 3 one can see that just above this energy the trend in the theoretical results start to deviate from the experimental data.

The lower panel of Fig. 3 shows a zoom of the top panel. This was considered necessary since the present theoretical results span a range of four orders of magnitude in energy and more than three orders of magnitude in cross section, while the experimental results cover a smaller energy and cross-section range. This figure shows that the experimental results generally agree well with each other above ∼7 eV. We see good accord between the present measurements and those of Floeder *et al*. [8], within the combined total error bars (not plotted), even down to 5 eV. However, the present data and that of Sueoka and Mori [9] differ considerably at smaller energies (<7 eV), where our data presents a sharp increase in magnitude when compared to that earlier measurement. We believe that this discrepancy is mainly due to the different angular discrimination (which is energy dependent) of the experiments. As the Trento apparatus has a superior angular resolution [3] compared to that of the spectrometer used by Sueoka and Mori [9] (see Sec. II), the forward angle scattering error is smaller in the present study compared to that in the earlier experiment. It is noticeable that the measurements of Sueoka and Mori [9] show clearly the onset of the positronium channel, unlike our measurements. Both discrepancies can be explained if we take into account the lower angular resolution of the Japanese apparatus. This difference has already been noted in our previous papers [3,33]. The two data sets can be brought into qualitative accord if we consider that the angular resolution error in the measurements of Sueoka and Mori increases towards the lower energies: The "non-positronium cross section" is depressed more than the positronium contribution in the range spanning 3.7–7 eV.

The low-energy behavior of the present experimental TCS is consistent with the trend in the theoretical curves present in the literature and with our most recent calculations. The current ICS agrees almost perfectly with the results from Occhigrossi and Gianturco [12], lying between the current experiment and the data from Sueoka and Mori [9], and being slightly higher than the previous calculations from da Silva *et al*. [10]. Our new ICS, however, becomes higher in magnitude than the present measurements at 0.4 eV. Although unexpected, this fact can be attributed to the energy convolution effect and forward angle scattering effect, leading to an underestimation of the experimental cross section.

The difference between the TCS and the elastic ICS from 0.5 to 3.7 eV (below the positronium channel threshold) could in principle arise from rovibrational excitations, not being taken into account in the theoretical calculations. For small molecules, the simple Born-dipole approximation provides fair estimates of $0 \rightarrow 1$ vibrational excitation cross sections for IR active modes [34]. Though not shown here, we obtained vibrational excitation cross sections for ethene in this fashion. As the molecule has a single strongly IR active vibration, namely the ν_7 mode with $\hbar\omega = 0.118$ eV [35], the vibrationally inelastic cross section, as obtained from the sum of $0 \rightarrow 1$ excitations of IR active modes, would provide a minor contribution to the TCS (∼2.5%) below the Ps formation threshold. However, the Born-dipole approximation cannot account for the vibrational couplings arising from virtual state formation. It is a well-known fact in the electron scattering community [36], later also shown for positron scattering [37], that vibrational excitation cross sections can be greatly enhanced at threshold due to the presence of a virtual state. Although no simple approximation would allow for a reliable description of this effect, one could expect significant vibrational excitation based on the one-to-one correspondence between resonances in the annihilation rate and in the vibrationally summed cross section discussed elsewhere [15]. As annihilation measurements for ethene [38] indicate the coupling of IR active and inactive modes, as well as overtones and combination modes, signatures of these vibrations should also be present in the scattering cross section. This could explain, at least in part, the difference between the

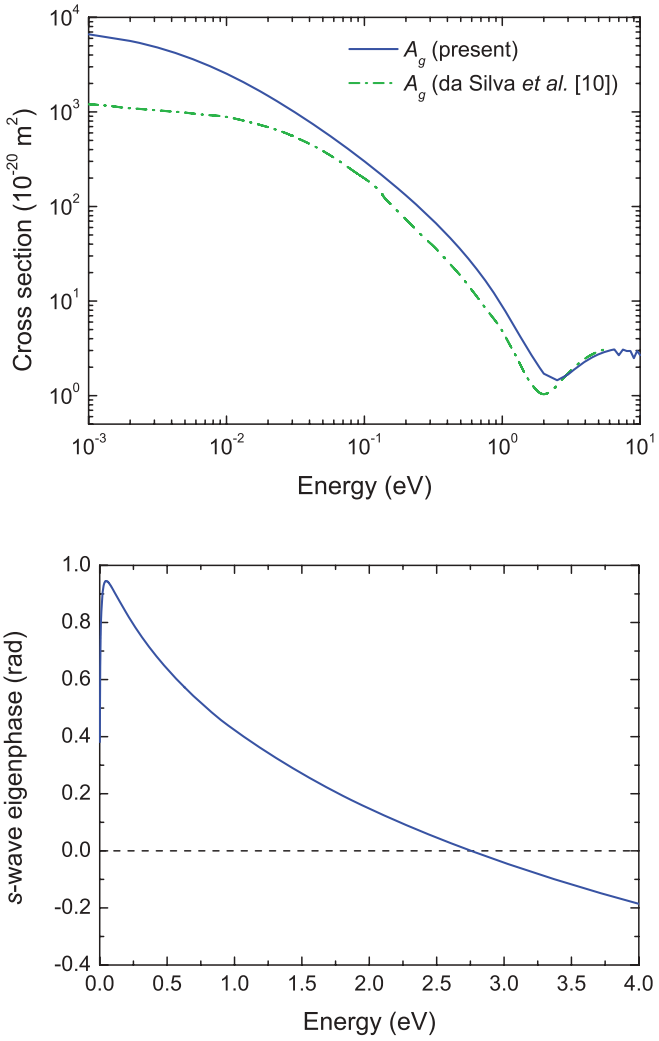

FIG. 4. (Color online) (Upper panel) Elastic ICS for the A_g symmetry. Solid line (blue), present results; dot-dashed line (green), results from [10]. (Lower panel) s-wave eigenphase corresponding to the present calculations. See text for discussion.

measured TCS and the calculated elastic ICS at the lower energies.

The behavior of our measured and computed cross sections at very low energy is consistent with the presence of a virtual state, as was seen in [4]. We show in Fig. 4 the cross section for the A_g symmetry of the D_{2h} group and the s-wave eigenphase. We also show the A_g cross section of da Silva *et al.* [10]. Our present results clearly show the presence of a virtual state, indicated by a sharp increase of the cross section and by the s-wave eigenphase. According to the Levinson's theorem [39], in an ideal scenario (virtual state at $E = 0$), as the energy goes to zero, the s-wave eigenphase should go to $\pi/2$. In real situations, the virtual state is slightly shifted from zero energy (into the negative imaginary axis of the complex momentum plane), such that the eigenphase drops to zero after approaching $\pi/2$, as $E \to 0$ [40]. We calculated the scattering length with the procedure suggested by Morrison [41] and obtained the value of $-47.76\,a_0$ (a_0 is the Bohr radius and $1a_0 = 0.52918 \times 10^{-10}$ m), which confirms the presence of a virtual state. This value is more than twice as large as the scattering length of $-18.5\,a_0$ obtained by Ref. [42], estimated from the data of da Silva *et al.* [10]. We also observe that the Ramsauer-Townsend minimum in the A_g cross section is shifted to a higher energy compared to the previous calculation [10]. This is consistent with the improved description of polarization effects in the present calculation and can also be observed in the s-wave eigenphase, as it crosses zero at around 2.8 eV. This crossing is a result of the interaction potential between the positron and the target, which is a sum of the Coulomb (repulsive) and the polarization (attractive) potentials. At low energy, the polarization interaction dominates, and the positron feels a net attractive potential. As the energy increases, the Coulomb potential becomes more important, and the positron feels a net repulsive potential. As a consequence, the potential changes sign (crossing zero) when going from an attractive to a repulsive potential.

V. SUMMARY

We presented experimental and calculated cross sections for positron collisions with ethene. The current experimental total cross sections agree well with previous experimental data for energies above 7 eV. Below this energy some differences in magnitude are observed, as our current results greatly increase in value compared to the data of Sueoka and Mori [9] for lower energies. Such discrepancies can, however, be understood in terms of the superior angular discrimination of the Trento apparatus compared to that from the Japanese group. The calculated cross sections agree relatively well with the experimental data, and show a very good agreement with previous theoretical results. In particular, the elastic cross section shows the presence of a virtual state, consistent with the experimental observation at lower energies, and also of a Ramsauer-Townsend minimum at around 2.8 eV.

ACKNOWLEDGMENTS

S.d'A.S. and M.H.F.B. acknowledge support from CNPq, FINEP (under project CT-Infra) and from Fundação Araucária. M.T.doN.V. and M.A.P.L. acknowledge support from CNPq and FAPESP. S.d'A.S. and M.H.F.B acknowledge computational support from Carlos M. de Carvalho at DFis-UFPR and at LCPAD-UFPR. The authors also acknowledge computational support from CENAPAD-SP. This work was also conducted under a Memorandum of Understanding between the University of Trento and the Flinders University node of the Australian Research Council Centre for Antimatter-Matter Studies.

[1] C. M. Surko, G. F. Gribakin, and S. J. Buckman, J. Phys. B **38**, 567R (2005).

[2] See, for instance, S. d'A. Sanchez, F. Arretche, and M. A. P. Lima, Phys. Rev. A **77**, 054703 (2008); A. Zecca, L. Chiari, E. Trainotti, D. V. Fursa, I. Bray, and M. J. Brunger, Eur. Phys. J. D **64**, 317 (2011).

[3] A. Zecca, L. Chiari, A. Sarkar, and M. J. Brunger, New J. Phys. **13**, 115001 (2011).

[4] A. Zecca, L. Chiari, E. Trainotti, A. Sarkar, S. d'A. Sanchez, M. H. F. Bettega, M. T. do N. Varella, M. A. P. Lima, and M. J. Brunger, Phys. Rev. A **85**, 012707 (2012).

[5] B. M. Bode and M. S. Gordon, J. Mol. Graphics Modell. **16**, 133 (1998).

[6] See, for instance, L. M. Brescansin, L. E. Machado, and M. T. Lee, Phys. Rev. A **57**, 3504 (1998); R. Panajotovic, M. Kitajima, H. Tanaka, M. Jelisavcic, J. Lower, L. Campbell, M. J. Brunger, and S. J. Buckman, J. Phys. B **36**, 1615 (2003); C. S. Trevisan, A. E. Orel, and T. N. Rescigno, Phys. Rev. A **68**, 062707 (2003); C. Winstead, V. McKoy, and M. H. F. Bettega, *ibid.* **72**, 042721 (2005), and references therein.

[7] R. F. da Costa, M. H. F. Bettega, and M. A. P. Lima, Phys. Rev. A **77**, 042723 (2008); M. Allan, C. Winstead, and V. McKoy, *ibid.* **77**, 042715 (2008).

[8] K. Floeder, D. Fromme, W. Raith, A. Schwab, and G. Sinapius, J. Phys. B **18**, 3347 (1985).

[9] O. Sueoka and S. Mori, J. Phys. B **19**, 4035 (1986).

[10] E. P. da Silva, J. S. E. Germano, and M. A. P. Lima, Phys. Rev. Lett. **77**, 1028 (1996).

[11] J. Sun, G. Yu, Y. Jiang, and S. Zhang, Eur. Phys. J. D **4**, 83 (1998).

[12] A. Occhigrossi and F. A. Gianturco, J. Phys. B **36**, 1383 (2003).

[13] E. P. da Silva, J. S. E. Germano, J. L. S. Lino, C. R. C. de Carvalho, A. P. P. Natalense, and M. A. P. Lima, Nucl. Instrum. Methods Phys. Res. Sect. B **143**, 140 (1998).

[14] J. A. Young, G. F. Gribakin, C. M. R. Lee, and C. M. Surko, Phys. Rev. A **77**, 060702(R) (2008).

[15] S. d'A. Sanchez, M. A. P. Lima, and M. T. do N. Varella, Phys. Rev. A **80**, 052710 (2009).

[16] S. d'A. Sanchez, M. A. P. Lima, and M. T. do N. Varella, Phys. Rev. Lett. **107**, 103201 (2011).

[17] J. S. E. Germano and M. A. P. Lima, Phys. Rev. A **47**, 3976 (1993).
[18] E. P. da Silva, J. S. E. Germano, and M. A. P. Lima, Phys. Rev. A **49**, 1527R (1994).
[19] A. Zecca, L. Chiari, A. Sarkar, S. Chattopadhyay, and M. J. Brunger, Nucl. Instrum. Methods Phys. Res. Sect. B **268**, 533 (2010).
[20] A. Zecca, L. Chiari, E. Trainotti, D. V. Fursa, I. Bray, A. Sarkar, S. Chattopadhyay, K. Ratnavelu, and M. J. Brunger, J. Phys. B **45**, 015203 (2012).
[21] A. Zecca, L. Chiari, E. Trainotti, D. V. Fursa, I. Bray, and M. J. Brunger, Eur. Phys. J. D **64**, 317 (2011).
[22] A. Zecca, L. Chiari, E. Trainotti, and M. J. Brunger, J. Phys. B **45**, 085203 (2012).
[23] A. Zecca and M. J. Brunger, in *Nanoscale Interactions and Their Applications: Essays in Honour of Ian McCarthy*, edited by F. Wang and M. J. Brunger (Research Signpost, Trivandrum, India, 2007), p. 21.
[24] T. Takaishi and Y. Sensui, Trans. Faraday Soc. **59**, 2503 (1963).
[25] J. P. Sullivan, C. Makochekanwa, A. Jones, P. Caradonna, D. S. Slaughter, J. Machacek, R. P. McEachran, D. W. Mueller, and S. J. Buckman, J. Phys. B **44**, 035201 (2011).
[26] W. E. Kauppila, T. S. Stein, J. H. Smart, M. S. Dababneh, Y. K. Ho, J. P. Downing, and V. Pol, Phys. Rev. A **24**, 725 (1981).
[27] J. R. Machacek, C. Makochekanwa, A. C. L. Jones, P. Caradonna, D. S. Slaughter, R. P. McEachran, J. P. Sullivan, S. J. Buckman, S. Bellm, B. Lohmann, D. V. Fursa, I. Bray, D. W. Mueller, and A. D. Stauffer, New J. Phys. **13**, 125004 (2011).
[28] A. Hamada and O. Sueoka, J. Phys. B **27**, 5055 (1994).
[29] K. Takatsuka and V. McKoy, Phys. Rev. A **24**, 2473 (1981); **30**, 1734 (1984).
[30] A. Zecca, E. Trainotti, L. Chiari, M. H. F. Bettega, S. d'A. Sanchez, M. T. do N. Varella, M. A. P. Lima, and M. J. Brunger, J. Chem. Phys. **136**, 124305 (2012).
[31] W. J. Hunt and W. A. Goddard III, Chem. Phys. Lett. **3**, 414 (1969).
[32] F. Z. Chen and C. Y. Robert Wu, J. Phys. B **32**, 3283 (1999).
[33] A. Zecca, L. Chiari, E. Trainotti, A. Sarkar, and M. J. Brunger, PMC Physics B **3**, 4 (2010).
[34] J. P. Marler, G. F. Gribakin, and C. M. Surko, Nucl. Instrum. Methods Phys. Res. Sect. B **247**, 87 (2006).
[35] D. M. Bishop and L. M. Cheung, J. Phys. Chem. Ref. Data **11**, 119 (1982).
[36] R. K. Nesbet, Phys. Rev. A **19**, 551 (1979); J. P. Gauyacq and A. Herzenberg, *ibid.* **25**, 2959 (1982); W. Domcke, J. Phys. B **14**, 4889 (1981); H. Estrada and W. Domcke, *ibid.* **18**, 4469 (1985).
[37] T. Nishimura and F. A. Gianturco, Phys. Rev. A **72**, 022706 (2005); E. M. de Oliveira, M. A. P. Lima, S. d'A. Sanchez, and M. T. do N. Varella, *ibid.* **81**, 012712 (2010).
[38] S. J. Gilbert, L. D. Barnes, J. P. Sullivan, and C. M. Surko, Phys. Rev. Lett. **88**, 043201 (2002); L. D. Barnes, S. J. Gilbert, and C. M. Surko, Phys. Rev. A **67**, 032706 (2003).
[39] C. J. Joachaim, *Quantum Collision Theory* (North Holland, Amsterdam, 1975).
[40] C. R. C. de Carvalho, M. T. do N. Varella, M. A. P. Lima, and E. P. da Silva, Phys. Rev. A **68**, 062706 (2003).
[41] M. A. Morrison, Phys. Rev. A **25**, 1445 (1982).
[42] G. F. Gribakin, Phys. Rev. A **61**, 022720 (2000).